

# Assessment of the Electric Field Induced by Deep Transcranial Magnetic Stimulation in the Elderly Using H-Coil

Serena Fiocchi<sup>1</sup>, Yiftach Roth<sup>2</sup>, Abraham Zangen<sup>2</sup>, Paolo Ravazzani<sup>1</sup>,  
and Marta Parazzini<sup>1</sup>

<sup>1</sup>Consiglio Nazionale delle Ricerche

Istituto di Elettronica e di Ingegneria dell'Informazione e delle Telecomunicazioni, Milan, 20133, Italy  
serena.fiocchi@ieiit.cnr.it, paolo.ravazzani@ieiit.cnr.it, marta.parazzini@ieiit.cnr.it

<sup>2</sup>Department of Life Sciences

Ben-Gurion University of the Negev, Be'er Sheva, 84105, Israel  
yiftah@Brainsway.com, azangen@bgu.ac.il

**Abstract** — The recent advancements in the design of TMS coils to reach specific cortical and subcortical regions have allowed the treatment of various neuropsychiatric disorders, whose prevalence increases with age. This could be also due to the anatomical and morphological changes with age of the brain tissues, such as the atrophy that characterizes the elderly cortex. This study provides a description of the electric field, the main engine of the stimulation, distribution induced in specific cerebral tissues. That was performed by comparing, making use of computational electromagnetic techniques, the  $\mathbf{E}$  distributions in two human models of different ages (34 and 84 years-old males), the older one showing cortical atrophy in the prefrontal lobe. The analysis of the parameters describing the spread of the electric field distribution shows that the H1 coil is able to induce in the prefrontal cortex an  $\mathbf{E}$  amplitude higher than the neural threshold and with a widespread distribution in both models, with a slight prevalence on the younger one. On the contrary, the maximum  $\mathbf{E}$  penetration depth and the consequent capability to reach deeper targets in the brain, is slightly higher for the elderly model.

**Index Terms** — Bioelectromagnetics, deep transcranial magnetic stimulation, elderly, H-coils, neuropsychiatric disorders.

## I. INTRODUCTION

In the last few years, the possibility to approach the treatment of pathological conditions with noninvasive techniques of neurostimulation, such as transcranial magnetic stimulation TMS and transcranial direct current stimulation tDCS, has become more and more appealing to neuroscientists. In parallel, their use moved from the merely diagnosis of damage, to the therapy of

many neuropsychiatric disorders and spinal injuries [1]-[8]. The efficacy of these techniques is associated to the induction of electric field ( $\mathbf{E}$ ), which acts by modulating the electrical activity of the target neural region of interest. That can take place in a direct way as in transcranial electrical stimulation, through electrodes placed over the skin close to the target of interest, or else in an indirect way as in the case of TMS, through coils placed in proximity to the scalp.

Lately, the knowledge of the role of different cortical and subcortical structures in the development of specific neuropsychiatric pathologies has moved the interest of researchers to develop new TMS coils able to stimulate deep brain structures rather than only the cortex, giving birth to the deep TMS (dTMS). For example, in the major depressive disorder (MDD), some functional neuroimaging studies have shown the presence of alterations in the prefrontal cortex (PFC) and in areas belonging to the reward circuit linked with the dorsal and ventral lateral PFC, i.e., the nucleus accumbens and the ventral tegmental area [9,10]. The dorsolateral prefrontal cortex (DLPFC) was found to be critically involved in both mood and reward mechanisms and was found to be dysfunctional in both MDD and substance-abuse patients [11]-[13]. Also, it was indicated, together with the hippocampus, as the dTMS target for the treatment of schizophrenia [13] and of dysthymic disorder [15]. The medial prefrontal cortex (MPFC) was identified as target region for the treatment of the post-traumatic stress disorder [16]. The role of the PFC in the regulation of mood and anxiety was confirmed by a study in which repetitive TMS of the right DLPFC was associated with disrupted PFC-amygdala connectivity [17]. Lastly, it is well known that midbrain and subthalamic structures are strictly involved in the progress of subcortical dementias, such as Parkinson disease

(PD), Huntington’s disease and vascular dementia [18].

Many of these pathologies also affect elderly people, that present a prefrontal atrophy related to the age [19], and hence, in these patients, the capability to effectively reach deeper brain regions could be even more critical.

dTMS is administered by specific coils, designed at the precise scope to improve the penetration depth of the stimulation. Among those ones, the so-called Heschl family (H-) coils have been exploited in several studies [20]-[28] with significant outcomes. They have larger dimension with respect to the conventional TMS coils and a complex three-dimensional structure, which allows to minimize the non-tangential element in the coil and to slower the decay of electric field with distance.

Although these techniques are becoming more and more popular in neuroscience, little is known about the actual distribution of the  $\mathbf{E}$  field induced within the cerebral tissues by dTMS coil configurations. Although some estimations of the induced  $\mathbf{E}$  in dTMS have been performed in adult or in simplified models [30]-[33], so far, no investigation has addressed the issue of the  $\mathbf{E}$  distribution in elderly people.

This study, therefore, addresses precisely this topic through a computational approach. In detail, we assessed, by using numerical electromagnetic techniques, the  $\mathbf{E}$  distributions induced by a particular coil of the H-coil family (the H1 coil) in an anatomical head model of an 84 years old man with a pronounced age related prefrontal atrophy. Then it was compared with the  $\mathbf{E}$  distribution in an adult male model, stimulated with the same coil configuration. The purpose is to investigate and quantify the  $\mathbf{E}$  distributions in different brain regions in the elderly, with particular attention to the cerebral targets for the treatment of neuropsychiatric disorders, i.e., as stated above, the prefrontal cortex and related areas and the deeper tissues. The comparison with the stimulation of an adult head with identical coil configuration, will also allow exploring the change with age of the  $\mathbf{E}$  distribution.

## II. MATERIALS AND METHOD

A computational approach as implemented by the simulation platform SEMCAD X [34] was used to build the simulations and then to assess the distribution of the electric field  $\mathbf{E}$  inside specific brain target tissues. In detail, we used the magneto quasi-static low-frequency solver to solve the Biot-Savart law. It is based on the scalar potential finite element (SPFE) method. Since in the low frequency band, the appropriate dimensions of the computational domain are smaller than the free space wavelength, the magnetic vector potential  $\mathbf{A}$  is decoupled from  $\mathbf{E}$ . Given here the dominance in the human body of the conduction currents,  $\mathbf{E}$  can be calculated from the scalar potential  $\Phi$ , which is given by:

$$-\nabla \cdot \sigma \nabla \Phi = \mathbf{j} \omega \nabla \cdot (\sigma \mathbf{A}). \quad (1)$$

Simulations were conducted over two realistic anatomical models of the Virtual Population [35]. They are based on high-resolution magnetic resonance (MR) images of two volunteers (a 34 and a 84 years-old male adult models, named “Duke” and “Glenn”, respectively). Both models distinguish up to 84 tissues within the whole body and up to 20 different tissues at the head level. With the aim to analyse the induced  $\mathbf{E}$  distributions inside specific brain target areas, in both human models, we identified the prefrontal cortex (PFC), and within this, the dorsolateral prefrontal cortex (DLPFC) and the medial prefrontal cortex (MPFC), and the deeper neuronal regions of the reward-related pathways such as amygdala, nucleus accumbens and ventral tegmental area (VTA), by comparison with MR images based brain atlas.

To all the tissues we assigned the dielectric properties based on data at low frequency collected by the studies of Gabriel and colleagues [36], [37].

A hexahedral uniform meshing algorithm at 1 mm of resolution, performed by the computational software [34], was used to discretize the computational domain, limited to the upper region of the body at the shoulder level.

Among the Heschl coils family [38], we chose the H1 coil, recently used in some dTMS studies ([20]-[29]) for the treatment of neuropsychiatric diseases. It is built on a complex three-dimensional structure, which is supposed to reach the deep brain tissues as well as to enhance the PFC stimulation. In detail, it is composed of 12 windings that form a base portion, a protruding return portion and a contacting return portion, indicated as  $\alpha$ ,  $\beta$  and  $\gamma$  respectively in Fig. 1.

The base portion ( $\alpha$ ) has a curved shape along its length axis in order to wrap the subject’s scalp and it provides electrical current flow in a direction tangential to prefrontal and orbitofrontal regions [38]. The protruding ( $\beta$ ) and the contacting ( $\gamma$ ) return portions are arranged to carry returning current in a direction opposite to the one in the brain target area. The coil model was built to accommodate the anatomy of the head on which it is placed, as it happens during the experiments. The current flows clockwise and in the same direction in each winding. As to the coil positioning, we followed a procedure mimicking what is currently done in neurophysiological experiments making use of H-family coils for stimulating the PFC (see e.g., [13], [15], [22], [24]-[26], [28], [29]). For both human models, the coil was first placed on the scalp and the coil current at a frequency of 5 kHz was adjusted in order to achieve a level of  $\mathbf{E}$  equals to the 120 % of the motor threshold (i.e., in our case, 120 V/m, considering a threshold equals to 100 V/m) in the area of the motor cortex corresponding to the right hand abductor pollicis brevis (APB). The 100 V/m threshold (in the following identified as  $E_{th}$ ) was chosen according to the accepted

range of threshold required for hand motor activation. Secondly, the coil was moved 5.5 cm anteriorly to reach the prefrontal cortex, as shown in Fig. 1 for the model Glenn. With the purpose to describe the  $\mathbf{E}$  distribution amplitude, the results in the following section will be presented in terms of descriptive statistics of the  $\mathbf{E}$  amplitudes (median, 25<sup>th</sup> and 75<sup>th</sup> percentiles, minimum and maximum) in different brain regions. Moreover we also calculated the spread of the distribution in the PFC, DLPFC and MPFC by identifying the percentage of volume of these brain regions where the  $\mathbf{E}$  amplitude was equal or greater than 50%, 70%, 80%, 90% and 100% (in the following of the paper named as V50, V70, V80, V90 and V100) of  $E_{th}$  [30].

With the specific intent of quantifying the  $\mathbf{E}$  penetration depth reached in the frontal lobe of the two human models, we calculated the maximum depth of the point in the prefrontal lobe in which the induced  $\mathbf{E}$  amplitude was equal or greater than the 70% and the 100% of  $E_{th}$ . Briefly, we assumed a brain centre located in the midpoint between the two nuclei accumbens, to identify a direction of depth in the prefrontal lobe. Then, we calculated the maximum depth from the scalp, the cortex and the white matter of the closest point to this centre with an  $\mathbf{E}$  amplitude equal to or greater than 70 or 100%  $E_{th}$  along the depth direction (i.e., the one passing through the brain centre mentioned above and the identified point) For a schematic representation see the following Fig. 5 (a).

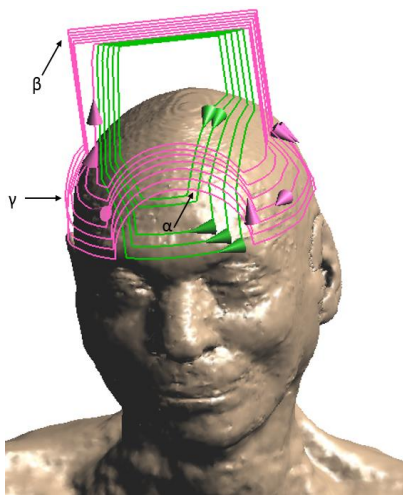


Fig. 1. Front view of H1 coil positioning on the head of model Glenn with the indication of the three portion described in the text: base portion ( $\alpha$ ), protruding return portion ( $\beta$ ), and contacting portion ( $\gamma$ ).

### III. RESULTS

Figure 2 shows the descriptive statistic (25<sup>th</sup>, 50<sup>th</sup>, 75<sup>th</sup> percentile, minimum and maximum) of the  $\mathbf{E}$  amplitude distributions induced in different brain

structures of the two human models. For both models, the maximum  $\mathbf{E}$  was found in the DPFC and equal to 222.4 V/m and 186.3 V/m for Duke and Glenn, respectively. It is worth noting that, as expected, the maximum  $\mathbf{E}$  amplitude has been found higher than the motor threshold  $E_{th}$  in various areas, e.g., over the cortex and the white matter and in all the regions of PFC.

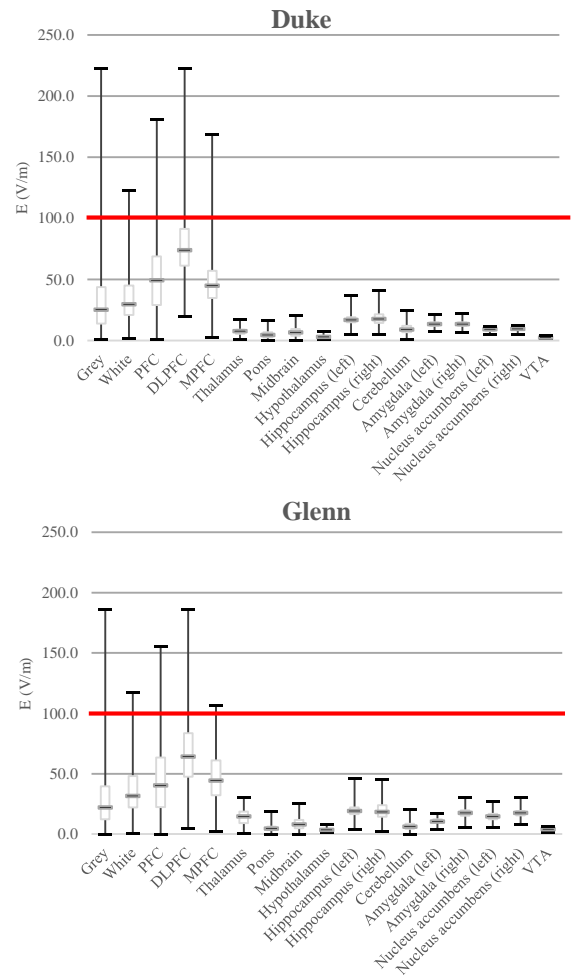


Fig. 2. Descriptive statistic of  $\mathbf{E}$  amplitude in different brain regions for both models. Red line marks the level of the motor threshold  $E_{th}$ .

On the contrary, in the deeper regions, the maximum  $\mathbf{E}$  amplitude remains always lower than the 50% of  $E_{th}$  (i.e., 50 V/m) in both models. The  $\mathbf{E}$  amplitude values on the cortex, the white matter, the PFC and its specific regions (DLPFC and MPFC), are slightly higher in Duke than in Glenn both in terms of median and maximum values, with differences in percentage, across the tissues, ranging from 16.1% to 58.5% in the maximum values and from 0.6% to 21.7% in the median values. On the contrary, the  $\mathbf{E}$  amplitude levels in the deep regions are slightly higher in Glenn than in Duke, with a maximum

difference of 88.6% in the median values and up to 94% in the peak values, across the different deep brain structures.

Figure 3 shows an example of  $E$  amplitude distributions on two coronal slices of the brain (grey and white matter) of Duke (on the left) and of Glenn (on the right).

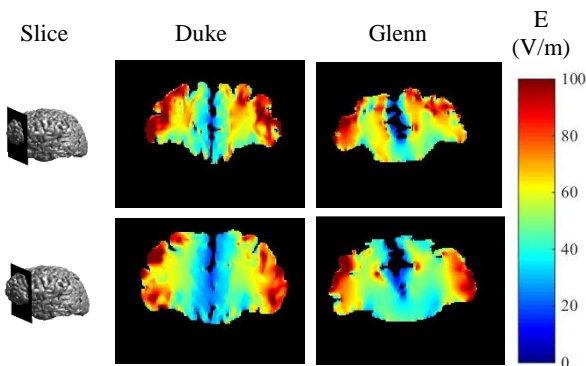


Fig. 3. Examples of  $E$  amplitude distributions on coronal slices of the brain of Duke (left) and of Glenn (right). The 1<sup>st</sup> column shows the coronal planes (taken 2 cm and 3 cm from the extremity of the PFC) where the sections were calculated. The colour bar is clamped to  $E_{th}=100$  V/m.

The 1<sup>st</sup> column shows the coronal planes (taken at 2 cm and 3 cm from the frontal extremity of the PFC) where the sections were calculated. The colour bar is clamped at  $E_{th}$ . The panels clearly show that the H1 coil can induce an  $E$  amplitude value higher than  $E_{th}$  in a large part of the prefrontal cortex and in both hemispheres. Moreover, as one can note, it is also able to reach wider and deeper regions of the brain with  $E$  amplitude values greater than 50% of  $E_{th}$  in both human models. The different morphology of the brain, due to the different age, seems to affect both the focality and the amplitude of the distribution.

In order to better quantify the spread of the  $E$  amplitude distributions, Fig. 4 shows the percentages of volume (V50, V70, V80, V90 and V100) of PFC (left or right), DLPFC (left or right) and MPFC where the  $E$  amplitude is equal or greater than a certain percentage of  $E_{th}$  for both human models. The figure clearly shows that the H1 coil is able to induce  $E$  amplitude values above  $E_{th}$  in a not negligible percentage of volume of the DLPFC, where it can reach up to 21% of the volume in the left DLPFC of Duke. More broadly, comparing the two human models, these percentages are slightly higher in Duke's DLPFC (both left and right) and left PFC, the average percentage increasing across V50-V100 in Duke of the 7.0%, 16.3% and 7.8% in left PFC, left DLPFC and right DLPFC, respectively. On the contrary, in the right PFC and MPFC these percentages instead remain

quantitatively comparable between the two human models with an average increase of 1.4% and 1.3% in Duke right PFC and MPFC, respectively.

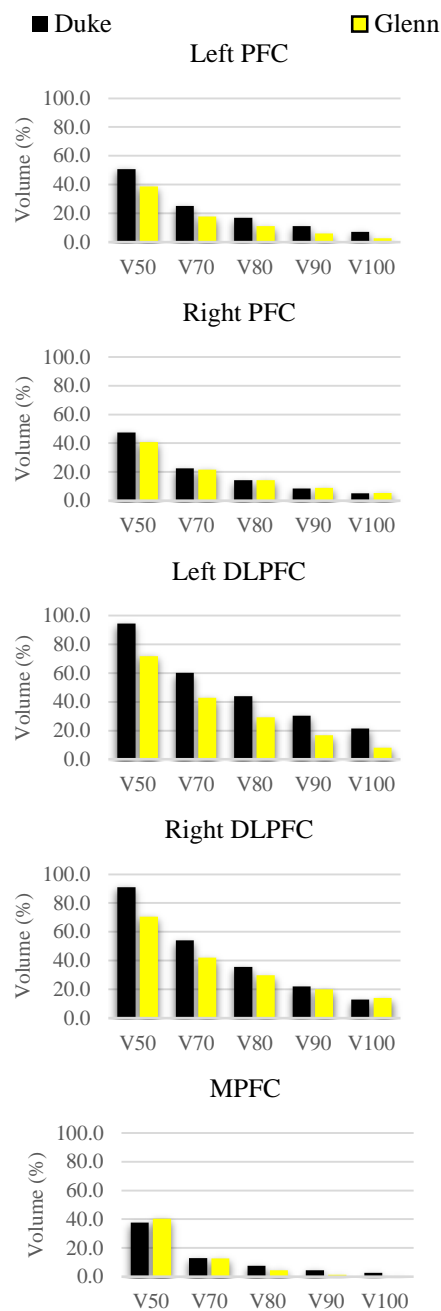


Fig. 4. Percentages of volume of PFC, DLPFC, both divided in the two cerebral hemispheres, and MPFC with  $E$  amplitude equals or greater than 50% (V50), 70% (V70), 80% (V80), 90% (V90) and 100% (V100) of  $E_{th}$  for Duke (black) and Glenn (yellow).

Figure 5 summarizes the penetration depths calculated from the scalp, the cortex and the white matter

in the two models, with respect to the brain centre (in the figure a pictorial description of the brain centre identification is also shown). We can notice that in both models the H1 coil is able to penetrate the cortex up to 3.9 cm with an  $E$  amplitude higher than the 70% of the neural threshold and up to 2.8 cm with an  $E$  amplitude above the neural threshold. Moreover, the H1 coil seems to be able to penetrate in the white matter with an  $E$  amplitude value above the neural threshold for approximately 2-2.5 cm. These penetration depths have been found always higher for Glenn.

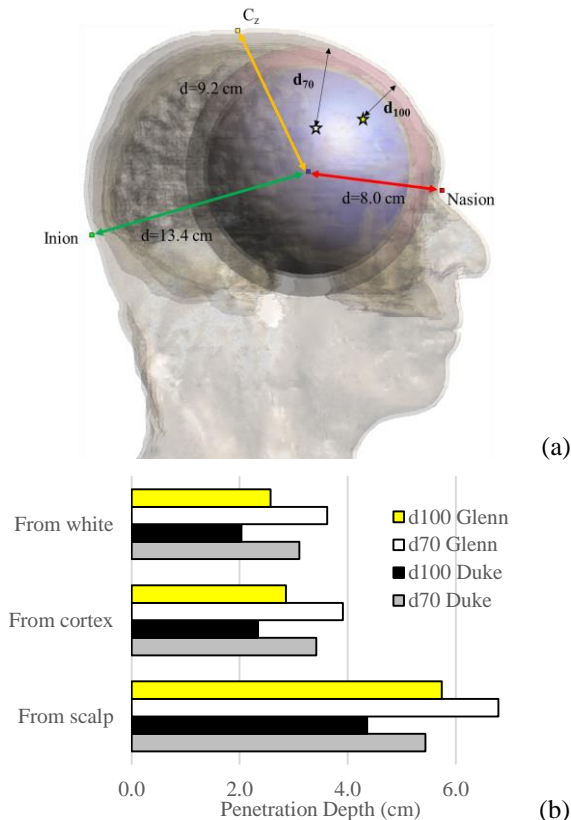


Fig. 5. (a) Pictorial representation of the penetration depth calculation from the surface of the scalp (taken as an example) over Glenn model. (b) Three-dimensional depth (cm) of the deepest point at 70% and at 100% of  $E_{th}$  (100 V/m) from the surface of the scalp, of the cortex and of the white matter of Duke and Glenn.

#### IV. DISCUSSION AND CONCLUSIONS

Although the recent application of dTMS for the treatment of neuropsychiatric disorders have attained significant outcomes, there is still a paucity of studies dedicated at a detailed description of the electric field distribution induced by coils specifically designed for dTMS. The very few studies that have recently addressed this topic [30]-[33], have used very simplified head models, such as spheres or have analysed just one

subject, mainly adult. In particular, no study has previously addressed the estimation of the  $E$  distributions in models of elderly people, for whom the presence of atrophy, due to the age, in the prefrontal area (one of the target of the stimulation for neuropsychiatric disorders), could modify the field distribution, and hence the treatment efficacy. In this study, we therefore have compared the  $E$  distributions in cerebral structures, typically target of dTMS by H-family coils, in two human models of 34 and 84 years old, respectively. The results of this study show that the maxima levels of the electric field are located mainly over the whole prefrontal cortex, the two dorsolateral prefrontal cortices and the medial prefrontal cortex, disregarding the age. These values can be noticeably higher than the motor threshold (see e.g., Fig. 2).

However, the anatomical variability affects directly both the levels of the fields in the PFC (Fig. 2), with a consistent decrease in the median and peak levels for the elderly model, and the field distribution (Fig. 3).

This could be due to the age related prefrontal atrophy that affects this latter model. Indeed, the distance between scalp and cortex equals to 20 mm in Duke against 29 mm in Glenn and the grey thickness in the prefrontal lobe is 3.1 mm in Duke, against 2.9 mm in Glenn. That age-effect is less evident if we compare the median levels over the entire cortex, it disappears in the white matter, and it reverses the trend in the subcortical regions, as a function of the reduction of the anatomical differences between the subjects.

The capability to reach deeper targets in the brain is higher for the elderly model, with an  $E$  amplitude below the 50% of the neural threshold (Fig. 2 and Fig. 5).

The maxima levels of  $E$  have been found in the two DLPFC, both in terms of field amplitude (Fig. 2) and spread of the distribution (Fig. 4), for both models. Indeed, almost the whole volume of DLPFC (90-94%, in the right and left DLPFC respectively) in the younger model and about the 70% in the older one, are above the 50% of  $E_{th}$  and a consistent volume across the models (10-20%) is above the neural threshold (see Fig. 4). These data could results of great interest in the clinical use of dTMS H1 coil, since those regions, as mentioned in the introductory section above, are strictly involved in the treatment of schizophrenia [14], dysthymia [15] and major depression [27]. The data about the spread (Fig. 4) show a slight effect of laterality in the stimulation of the DLPFC, with a prevalence for the left hemisphere (21% of the left DLPFC volume versus 13% of the right DLPFC volume above the neural threshold). This has been found in both models with a slight increase in the younger one. These results are in agreement with recent studies, which found the major depressive disorder associated with a decrease activity of the left DLPFC [39], [40].

As to the involvement of MPFC, Isseler and

colleagues [16] have indicated that cortical area as the target region for the treatment of post-traumatic stress disorder. Interestingly, our results show that the H1 coils is able to induce in about the 40% of the volume of this region an  $E$  amplitude above 50% of  $E_{th}$  in both models. Therefore, the use of H1 coil could be advisable for the stimulation of this target, disregarding the age.

Literature studies [16]-[18] have highlighted the possible involvement of some subcortical structures, such as amygdala, hippocampus, thalamus, nucleus accumbens and ventral tegmental area, in circuits related to the growth of depression disorders. Moreover, it is well known that the subthalamic area is strictly linked to the treatment of Parkinson disease and other dementias. Our results demonstrate that H1 coil can reach these structures with an amplitude field of about 25%  $E_{th}$ , with a slight prevalence on the older model. In line with this finding, we found a major capability to penetrate the cortex and the white matter with an amplitude field higher than the 70% and 100% of  $E_{th}$  in the old model (Fig. 5). This trend could be properly linked to the different anatomy between the two subjects (including the different scalp-grey distance and grey thickness mentioned above, as well as the head diameter and the cortical folding). In particular it could suggest that if on one side the prefrontal cortex atrophy of elderly people is responsible of lower  $E$  amplitude values on the cortex, on the other side it could facilitate the selectively reaching of brain regions below the grey and the white matter, improving the efficacy of this technique.

In conclusion, our study demonstrates that dTMS administered by H1 coil is capable to induced high levels of electric field  $E$  in typical target areas of neuropsychiatric disorders, disregarding the age of the subject. However, one should take into account that the levels of  $E$  slightly decrease in the elderly, although the depth of penetration of the induced field increases. These results confirm that the description and the quantification in terms of amplitude, focality and penetration depth of the distribution of the  $E$  in different brain regions, as here presented, could be of great help in planning and optimizing the clinical protocols, and in evaluating the outcomes of therapeutic treatments of differently-aged patients.

#### ACKNOWLEDGMENTS

The authors wish to thank Schmid & Partner Engineering AG ([www.speag.com](http://www.speag.com)) for having provided the simulation software SEMCAD X.

A preliminary version of this study has been presented at the International Conference on Electromagnetics in Advanced Applications (ICEAA 2015) in Advanced Applications (ICEAA 2015) held in Turin on 2015, 7-11 September. [S. Fiocchi, M. Parazzini, I. Liorni, Y. Roth, A. Zangen, and P. Ravazzani, "Deep transcranial magnetic stimulation for the treatment of neuropsychiatric

disorders in elderly people: electric field assessment," ICEAA 2015 proceedings].

#### FINALCIAL DISCLOSURES

Prof. Zangen and Dr. Roth are inventors of the deep TMS technology and have financial interests in Brainsway, which produces the deep TMS H-coil systems. All the other authors have no potential conflicts of interest to be disclosed.

#### REFERENCES

- [1] P. M. Rossini, D. Burke, R. Chen, L. G. Cohen, Z. Daskalakis, R. Di Iorio, V. Di Lazzaro, F. Ferreri, P. B. Fitzgerald, et al., "Non invasive electrical and magnetic stimulation of the brain, spinal cord, roots and peripheral nerves: Basic principles and procedures for routine clinical and research application. An updated report from an I.F.C.N. Committee," *Clin. Neurophysiol.*, vol. 126, no. 6, pp. 1071-1107, 2015.
- [2] A. V. Chervyakov, A. Y. Chernyavsky, D. O. Sinitsyn, and M. A. Piradov, "Possible mechanisms underlying the therapeutic effects of transcranial magnetic stimulation," *Front Hum. Neurosci.*, vol. 9, no. 303, (14 pp.), 2015.
- [3] M. Hallett, "Transcranial magnetic stimulation: a primer," *Neuron.*, vol. 55, no. 2, pp 187-199, 2007.
- [4] A. R. Brunoni, M. A. Nitsche, N. Bolognini, M. Bikson, T. Wagner, L. Merabet, et al., "Clinical research with transcranial direct current stimulation (tDCS): challenges and future directions," *Brain Stimul.*, vol. 5, no. 3, pp. 175-195, 2012.
- [5] D. Meron, N. Hedger, M. Garner, and D. S. Baldwin, "Transcranial direct current stimulation (tDCS) in the treatment of depression: Systematic review and meta-analysis of efficacy and tolerability," *Neurosci. Biobehav. Rev.*, vol. 29, no. 57, pp. 46-62, 2015.
- [6] M. Parazzini, S. Fiocchi, I. Liorni, E. Rossi, F. Cogiamanian, M. Vergari, A. Priori, and P. Ravazzani, "Modelling the current density generated by transcutaneous spinal direct current stimulation (tsDCS)," *Clinical Neurophysiology*, vol. 125, no. 11, pp. 2260-2270, 2014.
- [7] J. Lüdemann-Podubecká, K. Bösl, S. Rothhardt, G. Verheyden, and D. A. Nowak, "Transcranial direct current stimulation for motor recovery of upper limb function after stroke," *Neurosci. Biobehav.*, vol. 47, pp. 245-259, 2014.
- [8] C. Krishnan, L. Santos, M. D. Peterson, and M. Ehinger, "Safety of noninvasive brain stimulation in children and adolescents," *Brain Stimul.*, vol. 8, no. 1, pp. 76-87, 2015.
- [9] P. O. Harvey, F. Van den Eynde, A. Zangen, and M. T. Berlim, "Neural correlates of clinical improvement after deep transcranial magnetic

- stimulation (DTMS) for treatment-resistant depression: A case report using functional magnetic resonance imaging," *Neurocase.*, vol. 21, no. 1, pp. 16-22, 2015.
- [10] E. J. Nestler, M. Barrot, R. J. Di Leone, A. J. Eisch, S. J. Gold, and L. M. Monteggia, "Neurobiology of depression," *Neuron.*, vol. 32, pp. 13-25, 2002.
- [11] C. Rapinesi, M. Curto, G. D. Kotzalidis, A. Del Casale, D. Serata, V. R. Ferri, S. Di Pietro, et al., "Antidepressant effectiveness of deep transcranial magnetic stimulation (dTMS) in patients with major depressive disorder (MDD) with or without alcohol use disorders (AUDs): a 6-month, open label, follow-up study," *J. Affect Disord.*, vol. 174, pp. 57-63, 2015.
- [12] T. Ye, J. Peng, B. Nie, J. Gao, J. Liu, Y. Li, G. Wang, X. Ma, K. Li, and B. Shan, "Altered functional connectivity of the dorsolateral prefrontal cortex in first-episode patients with major depressive disorder," *Eur. J. Radiol.*, vol. 81, pp. 4035-4040, 2012.
- [13] L. Moreno-López, E. A. Stamatakis, M. J. Fernández-Serrano, M. Gómez-Río, A. Rodríguez-Fernández, M. Pérez-García, and A. Verdejo-García, "Neural correlates of the severity of cocaine, heroin, alcohol, MDMA and cannabis use in polysubstance abusers: A resting-PET brain metabolism study," *PLoS One*, vol. 7, no. 6, pp. e39830 (6 pp).
- [14] Y. Levkovitz, L. Rabany, E. V. Harel, and A. Zangen, "Deep transcranial magnetic stimulation add-on for treatment of negative symptoms and cognitive deficits of schizophrenia: A feasibility study," *Int. J. Neuropsychopharmacol.*, vol. 14, no. 7, pp. 991-6, 2011.
- [15] C. Rapinesi, G. D. Kotzalidis, D. Serata, A. Del Casale, F. S. Bersani, A. Solfanelli, P. Scatena, R. N. Raccah, R. Brugnoli, V. Digiacomantonio, P. Carbonetti, C. T. Fensore, R. Tatarelli, G. Angeletti, S. Ferracuti, and P. Girardi, "Efficacy of add-on deep transcranial magnetic stimulation in comorbid alcohol dependence and dysthymic disorder: Three case reports," *Prim Care Companion CNS Disord.*, vol. 15, no. 1, pp. 21, 2013.
- [16] M. Isserles, A. Y. Shalev, Y. Roth, T. Peri, I. Kutz, E. Zlotnick, and A. Zangen, "Effectiveness of deep transcranial magnetic stimulation combined with a brief exposure procedure in post-traumatic stress disorder--a pilot study," *Brain Stimul.*, vol. 6, no. 3, pp. 377-383, 2013.
- [17] P. Zwanzger, C. Steinberg, M. A. Rehbein, A. K. Bröckelmann, C. Dobel, M. Zavorotnyy, K. Domschke, and M. Junghöfer, "Inhibitory repetitive transcranial magnetic stimulation (rTMS) of the dorsolateral prefrontal cortex modulates early affective processing," *Neuroimage.*, vol. 101, pp. 193-203, 2014.
- [18] M. Cantone, G. Di Pino, F. Capone, M. Piombo, D. Chiarello, B. Cheeran, G. Pennisi, and V. Di Lazzaro, "The contribution of transcranial magnetic stimulation in the diagnosis and in the management of dementia," *Clin. Neurophysiol.*, vol. 125, no. 8, pp. 1509-1532, 2014.
- [19] Z. Nahas, X. Li, F. A. Kozel, D. Mirzki, M. Memon, K. Miller, K. Yamanaka, B. Anderson, J. H. Chae, D. E. Bohning, J. Mintzer, and M. S. George, "Safety and benefits of distance-adjusted prefrontal transcranial magnetic stimulation in depressed patients 55-75 years of age: A pilot study," *Depress Anxiety*, vol. 19, pp. 249-256, 2004.
- [20] E. Onesti, M. Gabriele, C. Cambieri, M. Ceccanti, R. Raccah, G. Di Stefano, A. Biasiotta, A. Truini, A. Zangen, and M. Inghilleri, "H-coil repetitive transcranial magnetic stimulation for pain relief in patients with diabetic neuropathy," *Eur. J. Pain*, vol. 17, pp. 1347-1356, 2013.
- [21] F. Spagnolo, M. A. Volonté, M. Fichera, R. Chieffo, E. Houdayer, M. Bianco, E. Coppi, A. Nuara, L. Straffi, G. Di Maggio, L. Ferrari, D. Dalla Libera, S. Velikova, G. Comi, A. Zangen, and L. Leocani, "Excitatory deep repetitive transcranial magnetic stimulation with H-coil as add-on treatment of motor symptoms in Parkinson's disease: An open label, pilot study," *Brain Stimul.*, vol. 72, pp. 297-300, 2014 .
- [22] Y. Levkovitz, E. V Harel, Y. Roth, Y. Braw, D. Most, et al., "Deep transcranial magnetic stimulation over the prefrontal cortex: Evaluation of antidepressant and cognitive effects in depressive patients," *Brain Stimul.*, vol. 2, pp. 188-200, 2009.
- [23] Y. Levkovitz , A. Sheer, E. V. Harel, L. N. Katz, D. Most, A. Zangen, and M. Isserles, "Differential effects of deep TMS of the prefrontal cortex on apathy and depression," *Brain Stimul.*, vol. 4, no. 4, pp. 266-74, Oct. 2011.
- [24] M. Isserles, O. Rosenberg, P. Dannon, Y. Levkovitz, M. Kotler, F. Deutsch, B. Lerer, and A. Zangen, "Cognitive-emotional reactivation during deep transcranial magnetic stimulation over the prefrontal cortex of depressive patients affects antidepressant outcome," *J. Affect Disord.*, vol. 128, pp. 235-42, 2011.
- [25] O. Rosenberg, N. Shoenfeld, A. Zangen, M. Kotler, and P. N. Dannon, "Deep TMS in a resistant major depressive disorder: a brief report," *Depress Anxiety.*, vol. 25, pp. 465-469, 2010.
- [26] O. Rosenberg, Y. Roth, M. Kotler, A. Zangen, and P. Dannon, "Deep transcranial magnetic stimulation for the treatment of auditory hallucinations: A

- preliminary open-label study," *Ann Gen Psychiatry*, vol. 10:3, 6 pp., 2011.
- [27] E. V. Harel, L. Rabany, L. Deutsch, Y. Bloch, A. Zangen, and Y. Levkovitz, "H-coil repetitive transcranial magnetic stimulation for treatment resistant major depressive disorder: An 18-week continuation safety and feasibility study," *World J. Biol. Psychiatry*, vol. 15, pp. 298-306, 2014.
- [28] F. S. Bersani, N. Girardi, L. Sanna, L. Mazzarini, et al., "Deep transcranial magnetic stimulation for treatment-resistant bipolar depression: A case report of acute and maintenance efficacy," *Neurocase*, vol. 19, pp. 451-457, 2013.
- [29] E. V. Harel, A. Zangen, Y. Roth, I. Reti, Y. Braw, et al., "H-coil repetitive transcranial magnetic stimulation for the treatment of bipolar depression: An add-on, safety and feasibility study," *World J. Biol. Psychiatry*, vol. 12, pp. 119-126, 2011.
- [30] V. Guadagnin, M. Parazzini, S. Fiocchi, I. Liorni, and P. Ravazzani, "Deep transcranial magnetic stimulation: Modeling of different coil configurations," *IEEE Trans. Biomed. Eng.*, Epub ahead of print, Nov. 6, 2011.
- [31] Y. Roth, A. Amir, Y. Levkovitz, and A. Zangen, "Three-dimensional distribution of the electric field induced in the brain by transcranial magnetic stimulation using figure-8 and deep H-coils," *Journal of Clinical Neurophysiology*, vol. 24, pp. 31-38, 2007.
- [32] Z. D. Deng, S. H. Lisanby, and A. V. Peterchev, "Coil design considerations for deep transcranial magnetic stimulation," *Clin. Neurophysiol.*, vol. 125, pp. 1202-1212, 2014.
- [33] Z. D. Deng, S. H. Lisanby, and A. V. Peterchev, "Electric field depth-focality tradeoff in transcranial magnetic stimulation: Simulation comparison of 50 coil design," *Brain Stimul.*, vol. 6, pp. 1-13, 2013.
- [34] SEMCAD X, Version 14.8 by SPEAG, Schmid & Partner Engineering, AG, Zurich, Switzerland, www.speag.com
- [35] A. Christ, W. Kainz, G. E. Hahn, K. Honegger, M. Zeffere, E. Neufeld, et al., "The virtual family-development of surface-based anatomical models of two adults and two children for dosimetric simulations," *Phys. Med. Biol.*, vol. 55, pp. N23-38, 2010.
- [36] S. Gabriel, R. W. Lau, and C. Gabriel, "The dielectric properties of biological tissues: II. measurements in the frequency range 10 Hz to 20 GHz," *Phys. Med. Biol.*, vol. 41, pp. 2251-2269, 1996.
- [37] C. Gabriel, A. Peyman, and E. H. Grant, "Electrical conductivity of tissue at frequencies below 1 MHz," *Phys. Med. Biol.*, vol. 54, pp. 4863-78, 2009.
- [38] A. Zangen, Y. Roth, P. C. Miranda, D. Hazani, and M. Hallet, "Transcranial magnetic stimulation, systems and methods," U.S. Patent 0288365, Nov. 24, 2011.
- [39] S. Grimm, J. Beck, D. Schuepbach, et al., "Imbalance between left and right dorsolateral prefrontal cortex in major depression is linked to negative emotional judgment: An fMRI study in severe major depressive disorder," *Biol. Psychiatry*, vol. 63, pp. 369-376, 2008.
- [40] M. Garcia-Toro, J. M. Montes, and J. A. Talavera, "Functional cerebral asymmetry in affective disorders: new facts contributed by transcranial magnetic stimulation," *J. Affect Disord.*, vol. 66, pp. 103-109, 2001.